J. Sens. Sens. Syst., 4, 263–269, 2015
www.j-sens-sens-syst.net/4/263/2015/
doi:10.5194/jsss-4-263-2015

JSSS Journal of Sensors and Sensor Systems Open Access

Ammonia storage studies on H-ZSM-5 zeolites by microwave cavity perturbation: correlation of dielectric properties with ammonia storage

M. Dietrich[1], D. Rauch[1], U. Simon[2], A. Porch[3], and R. Moos[1]

[1]Bayreuth Engine Research Center (BERC), Zentrum für Energietechnik (ZET), Department of Functional Materials, University of Bayreuth, 95440 Bayreuth, Germany
[2]Institute of Inorganic Chemistry (IAC), RWTH Aachen University, 52074 Aachen, Germany
[3]School of Engineering, Cardiff University, Cardiff CF24 3AA, Wales, UK

Correspondence to: M. Dietrich (functional.materials@uni-bayreuth.de)

Received: 5 June 2015 – Revised: 28 July 2015 – Accepted: 29 July 2015 – Published: 17 August 2015

Abstract. To meet today's emission standards, the ammonia-based selective catalytic reduction (SCR) has become the major NO_x control strategy for light and heavy diesel engines. Before NO_x reduction can proceed, adsorption of ammonia on the acidic sites of the catalyst is necessary. For improvements in efficiency and control of the exhaust gas aftertreatment, a better understanding of the ammonia storage on the acidic sites of zeolite-based SCR catalysts is needed. Thereby, the correlation of dielectric properties of the catalyst material itself with the ammonia storage is a promising approach. Recently, a laboratory setup using microwave cavity perturbation to measure the dielectric properties of catalyst material has been described. This study shows the first experimental data on zeolite-based SCR materials in their H-form. The SCR powder samples are monitored by microwave cavity perturbation while storing and depleting ammonia, both with and without admixed NO_x at different temperatures. Its complex dielectric permittivity is found to correlate closely with the stored mass of ammonia. The influence of the temperature and the Si / Al ratio of the zeolite to the ammonia storage behavior are also examined. These measurements disclose different temperature dependencies and differing sensitivities to ammonia storage for both real and imaginary parts of the complex permittivity. The apparent constant sensitivity of the real part can be related to the polarity of the adsorbed ammonia molecules, whereas the imaginary part depends on the Si / Al ratio and is related to the conductivity mechanisms of the zeolite material by proton hopping. It provides information about the zeolite structure and the number of (and the distance between) acidic storage sites, in addition to the stored ammonia mass.

1 Introduction

The stringent regulations for emissions of nitrogen oxides (NO_x) from combustion engines are a continuous factor in forcing automotive manufacturers to improve the efficiency of their exhaust gas aftertreatment systems. This is especially true for light- and heavy-duty diesel engines, which are operated leanly, where the ammonia-based selective catalytic reduction (SCR) has become the major NO_x control strategy to meet emission standards like the upcoming Euro 6 (Johnson, 2009). Metal oxides like V_2O_5–WO_3–TiO_2 (VWT) were established as SCR catalysts, but as a consequence of their classification as being toxic and harmful for the environment, zeolites with active components like iron (Fe) and copper (Cu) have received more attention in the past years (Rahkamma-Tolonen et al., 2005; DiIorio et al., 2015). In automotive applications, the ammonia-based SCR uses a non-toxic, aqueous urea solution (AdBlue) as a reducing agent. The injected solution decomposes thermally to ammonia (NH_3) in the hot exhaust. An essential precondition for SCR reactions is a previous NH_3 adsorption on the acidic sites on the zeolite surface. This NH_3 storage mechanism also buffers against changes of flow and temperature in order to secure a permanent NO_x conversion. The catalyst reduces NO_x selectively

to nitrogen (N_2) and water (H_2O). The two main SCR reactions are shown in the following: the standard SCR Reaction (R1) and the fast SCR Reaction (R2) with equimolar amounts of NO and NO_2 (Koebel et al., 2000):

$$4NH_3 + 4NO + O_2 \rightarrow 4N_2 + 6H_2O, \quad \text{(R1)}$$

$$4NH_3 + 2NO + 2NO_2 \rightarrow 4N_2 + 6H_2O. \quad \text{(R2)}$$

NH_3 storage capacity and catalytic activity of zeolite SCR catalysts depend on the number and strength of their acid sites (Lewis and Brønsted sites). NH_3 can adsorb strongly on Brønsted acid sites and weakly on top of each other on these sites via hydrogen bonds or on Lewis sites (Rodriguez-Gonzalez et al., 2008; Giodanino et al., 2014). Both acidic sides can be determined by temperature-programmed desorption (TPD) of NH_3, but a direct differentiation between Lewis and Brønsted sites is still not possible (Niwa and Katada, 2013). Therefore, the ability to measure dielectric properties under reaction conditions during NH_3 storage, and to correlate them with the catalytic behavior of the materials in situ, offers new opportunities to analyze and identify acidic sites and to optimize the catalyst material in general. Similarly, the NH_3 storage on SCR active materials has been investigated under defined gas atmospheres by impedance spectroscopy in a frequency range from 0.1 Hz to 1 MHz (Franke and Simon, 2004; Rodríguez-González et al., 2008). NH_3 loading and TPD experiments were performed with zeolite powders deposited on interdigitated capacitor chips to evaluate mechanistic models of proton transport in zeolites. In comparison with such impedance methods, the cavity perturbation method, which uses microwaves in the GHz range and a metal cavity resonator, holds promise for additional information and applications, not least because it is non-invasive (apart from interaction with a low power microwave field) and contactless.

Recently, a similar approach has been suggested and serial-type catalyst devices (as applied in automotive exhaust gas aftertreatment systems) have been examined (Moos et al., 2013). The catalytic converter had a volume of about 1.5 to 2 L. Since the sample occupied most of the cavity volume (metal canning), these systems are suitable for real-world applications but not to characterize material properties owing to their very large perturbation of the sample on the cavity space, making the inversion analysis for extracting complex permittivity very difficult. Instead, they are intended to detect the status of full-sized exhaust gas aftertreatment devices during operation on the road. Typical applications are the determination of the oxygen loading of three-way catalytic converters (Moos et al., 2008, 2013; Beulertz et al., 2013; Reiß et al., 2011a), or the soot loading (Sappok et al., 2010; Feulner et al., 2013) or ash loading (Kulkarni et al., 2013) of full-sized diesel particulate filters. The storage degree of NO in lean NO_x traps (Fremerey et al., 2011; Moos et al., 2009) and the NH_3 loading on SCR catalyst devices have also been successfully monitored (Reiß et al., 2011b; Rauch et al., 2014, 2015) using the cavity perturbation method.

In order to determine the dielectric properties of a catalyst material in operando, we have developed a laboratory test setup for catalyst powder characterization under reaction conditions by microwave cavity perturbation (introduced in Dietrich et al., 2014). It enables direct measurement of the complex permittivity of catalytic powder samples undergoing gas storage and catalytic reactions in a defined gas atmosphere, with gas analyzers upstream and downstream of the catalyst sample. In its first version, it operates within a temperature range from room temperature (where usually no reactions occur) to 300 °C.

2 Microwave cavity perturbation

The microwave cavity perturbation technique uses electromagnetic standing waves (resonances) inside a defined, hollow metal canning. The presence of a small sample inside the cavity resonator leads to a perturbation of the electromagnetic field distribution. For a sample placed within a region of maximum electric field (and zero magnetic field), the resulting decrease of the resonance frequency and the increase of the 3 dB bandwidth (i.e., decrease of the quality factor Q) of the resonance curve are related to real and imaginary parts, respectively, of the complex dielectric permittivity $\varepsilon = \varepsilon_1 - j\varepsilon_2$ of the sample: the real part ε_1 (or, more properly, $\varepsilon_1 - 1$) quantifies the polarization of the material and the imaginary part ε_2 quantifies the dielectric loss. The setup, fully described in Dietrich et al. (2014), is designed to use the TM_{010} mode of a cylindrical cavity resonator because of its uniform electric field along its axis, where the sample is positioned. The resonant frequency of the TM_{010} mode is set to around 1.2 GHz by suitable choice of the inner cavity radius. On inserting the sample, the real part ε_1 of its permittivity leads to a change of the resonance frequency from f_0 to f_s and its imaginary part ε_2 to a change of the unloaded quality factor from Q_0 to Q_s. With the volume of the sample V_s and the mode volume of the resonator V_{eff} (which is the effective volume occupied by the electric field energy and depends on the particular cavity mode), the complex dielectric permittivity can be calculated using Eqs. (1) and (2) (Porch et al., 2012).

$$\frac{f_0 - f_s}{f_0} \approx (\varepsilon_1 - 1)\frac{V_s}{2V_{eff}} \quad (1)$$

$$\frac{1}{Q_s} - \frac{1}{Q_0} = \Delta\left(\frac{1}{Q}\right) \approx \varepsilon_2 \frac{V_s}{V_{eff}} \quad (2)$$

The mode volume V_{eff} for the TM_{010} mode is 26.9 % of the enclosed volume of the cylinder. It should be noted that the fundamental interaction of the material with the microwave electric field via the material's polarization is exactly the same as that in microwave heating applications, but in cavity perturbation the electric field levels are so low (with input

power typically 1 mW or 0 dBm) that there is negligible sample heating.

3 Experimental

The samples under investigation are H-ZSM-5 zeolites with different Si / Al ratios (27, 90, 200 and 800). The powders were kindly provided by Clariant International Ltd. For zeolites in their H-form, the charge compensating cations are simply protons and no active metal ions are present (Franke and Simon, 1999). The number of acidic sites of the zeolite is directly dependent to the Al content. All samples were weighed and their skeletal volumes were determined using a helium gas pycnometer. The powders were placed on a porous frit in an almost lossless quartz glass tube and were heated independently from the cavity by a flow of hot air. The TM_{010} cavity mode is excited inductively by means of two loop-terminated coaxial lines around the perimeter of the cavity, with suitably oriented loops. The cavity measurement has been improved by using active water cooling to reduce measurement errors as a result of a non-uniform cavity temperature.

The sequence of the NH_3 storage experiments was identical for all samples and is shown for an H-ZSM-5 zeolite with a Si / Al ratio of 27 at 250 °C in Figs. 1a and 2. Figure 1a represents raw data for one measurement at 250 °C with the resonance peak of the TM_{010} mode shown without sample (black), with sample (red) and with sample loaded with NH_3 (blue). These measurements are taken with a vector analyzer (Anritsu VNA Master MS2028B) and here we plot the transmitted voltage amplitude $|S_{21}|$ as a function of frequency, which is a measure of resonator impedance. The insertion of the sample into the cavity leads to a reduction in resonance frequency, but not to an increased bandwidth (or, equivalently, a reduction in transmitted power or Q factor). This demonstrates that the unloaded zeolites have inherent low microwave loss, i.e., small values of ε_2. On loading with NH_3, the resonant frequency shifts further downwards and the bandwidth increases due to the high inherent electric dipole moment of the ammonia molecule. The parameters considered for microwave analysis are shown in Fig. 1b: the resonance frequency with the sample f_s, the 3 dB (or "half-power") bandwidth BW and the peak height $|S_{21,\max}|$. To calculate ε_1 from Eq. (1), the resonance frequency shift is used, determined simply from a change in frequency of the peak's maximum. For the calculation of ε_2 by Eq. (2), the unloaded quality factor Q is required, from which the effects of cavity coupling have been removed. Our cavity is designed (and measured) to have symmetric coupling, i.e., equal inductive coupling strength at each of its two ports, so the coupling unloading process can be calculated using Eq. (3) (Porch et al., 2012).

$$Q = \frac{f}{\mathrm{BW}}\left(1 - 10^{-|S_{21,\max}|/20}\right), \tag{3}$$

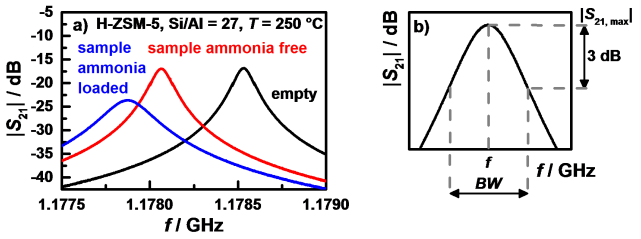

Figure 1. Example of a resonance curve of an H-ZSM-5 zeolite with Si / Al ratio of 27 at 250 °C: **(a)** the decrease of the resonance frequency from an empty sample tube (black) over a filled one without ammonia loading (red) to an ammonia loaded one (blue) can be clearly evaluated. The additional increase in bandwidth by ammonia loading is also visible. **(b)**: the resonance peak in more detail, showing the resonant frequency f, 3 dB bandwidth BW and maximum peak height $|S_{21,\max}|$.

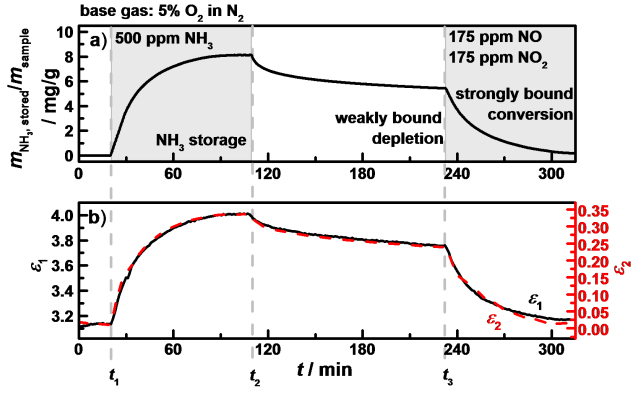

Figure 2. Experimental run for an H-ZSM-5 zeolite with a Si / Al ratio of 27 at 250 °C: **(a)** the stored amount of ammonia in the sample, and **(b)** the measured complex dielectric permittivity.

where the value of resonant frequency is f_0 for calculation of Q_0 (without the sample), or f_s for calculation of Q_s (with the sample).

Figure 2a shows the stored amount of NH_3 in the sample related to the sample mass, calculated from the difference between the measured upstream and downstream NH_3 concentrations. The results of the microwave measurements are displayed in Fig. 2b. The response of the material is immediate, but the response time of the measurement system is reduced by the acquisition time of the network analyzer, or more precisely, the time a frequency sweep requires. In the measurements shown in this paper, one frequency sweep took 75 s, but can be speeded up with different settings of the network analyzer. Initially, the samples were heated up to the measurement temperature in nitrogen with 5 % O_2 added with a total volume flow rate of 500 mL min^{-1}, leading to a mass-specific space velocity (WHSV) between 30 and 80 1 h^{-1}. At time t_1, 500 ppm NH_3 is admixed. The feed is stopped when the downstream gas analysis detected the inlet concentration (t_2), meaning that the catalyst powder is

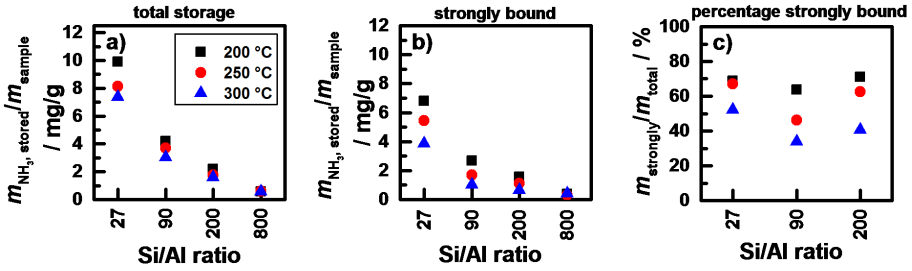

Figure 3. Ammonia storage behavior as a function of the Si / Al ratio at 200, 250 and 300 °C: **(a)** total storage, **(b)** strongly bound ammonia, and **(c)** percentage of strongly bound ammonia in relation to total storage.

saturated with NH_3 and the weakly bound NH_3 can desorb in the base gas. When no more NH_3 desorption can be detected downstream of the powder (t_3), the feed gas composition is changed to equimolar amounts of 175 ppm NO and 175 ppm NO_2 to convert the strongly bound NH_3 in the fast SCR Reaction (R2). At the end of each measurement run, the samples are again completely free of NH_3, as can be seen in the NH_3 balance and the microwave signal. It is clearly demonstrated in Fig. 2b that both the real part ε_1 (black) and imaginary part ε_2 (red dashed) of the complex dielectric permittivity are very strongly correlated to the mass of stored NH_3. This experiment was performed for each sample at temperatures of 200, 250 and 300 °C. In all experimental runs, no hints are found on sample degradation or deposition of unwanted reaction products, which could have either been detected by the gas analyzer, or would have led to visible changes of the powder samples.

4 Results and discussion

Before discussing the microwave measurement data, we first take a look at the storage behavior of the samples at different temperatures. Figure 3a shows the NH_3 mass at saturation (t_2 in Fig. 2) and Fig. 3b the strongly bound NH_3 after the free desorption (t_3 in Fig. 2) as a function of the Si / Al ratio at temperatures of 200, 250 and 300 °C. For comparison, the NH_3 mass is normalized to the mass of the examined sample powder. As expected, the total stored mass of NH_3 decreases with increasing temperature for all Si / Al ratios because of the temperature-dependent adsorption (Niwa and Katada, 2013). At 200 °C, the H-ZSM-5 zeolite with a Si / Al ratio of 27 is found to store 10 mg per gram of SCR sample, and with a Si / Al ratio of 800 less than 0.6 mg per gram of sample. The strongly bound NH_3 shows the same dependency on the Si / Al ratio and for a ratio of 27 the maximum storage of 7 mg/g is attained at a temperature of 200 °C. The calculated percentage of the strongly bound NH_3 is displayed in Fig. 3c for Si / Al ratios of 27, 90 and 200. The NH_3 mass for a ratio of 800 is too small for an accurate consideration. At 200 °C, the percentage of strongly bound NH_3 for the three considered samples is around 70 %, and at

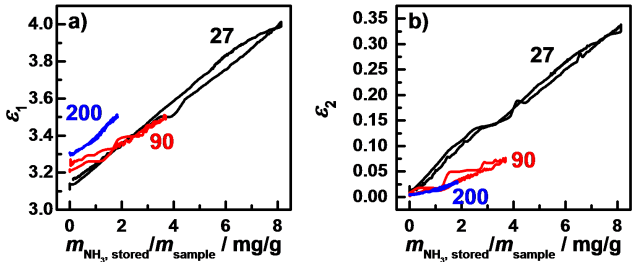

Figure 4. Measurement for an H-ZSM-5 zeolite with Si / Al ratios of 27 (black), 90 (red) and 200 (blue) at 250 °C: **(a)** ε_1 and **(b)** ε_2 as a function of the stored amount of ammonia in the samples.

300 °C between 35 and 50 %. These results indicate that the percentage of strongly bound NH_3 for HZSM-5 zeolites appears to be independent of the Si / Al ratio but dependent on temperature, as expected. Of course, the NH_3 mass for total and strongly bound storage is still a function of the number of storage sites and therefore a function of the Si / Al ratio.

Figure 4 shows the complex dielectric permittivity as a function of normalized stored NH_3 for Si / Al ratios of 27 (black), 90 (red) and 200 (blue) at 250 °C: (a) the real part ε_1 and (b) the imaginary part ε_2. In both plots, the entire measurement runs, including NH_3 loading, free desorption and SCR reaction, are displayed. It is clearly visible that a linear relation between the NH_3 loading and the complex permittivity occurs, regardless of whether the samples are storing or releasing NH_3. This basic behavior is observed in all measurements and indicates that both real and imaginary parts of the complex permittivity are suitable to detect NH_3 within zeolite-based SCR catalysts.

However, for some measurement runs the determined complex permittivity appear very noisy for the higher Si / Al ratios, generally as a result of lower NH_3 storage and higher sensitivity to small temperature changes. For an easier direct comparison of the observed samples, the following discussion is based on the permittivity values at three steady-state points of each measurement run (according to Fig. 2): the NH_3 free sample at the beginning of the measurement (t_1), total storage at saturation (t_2) and the remaining strongly bound NH_3 after free desorption (t_3). The results for Si / Al

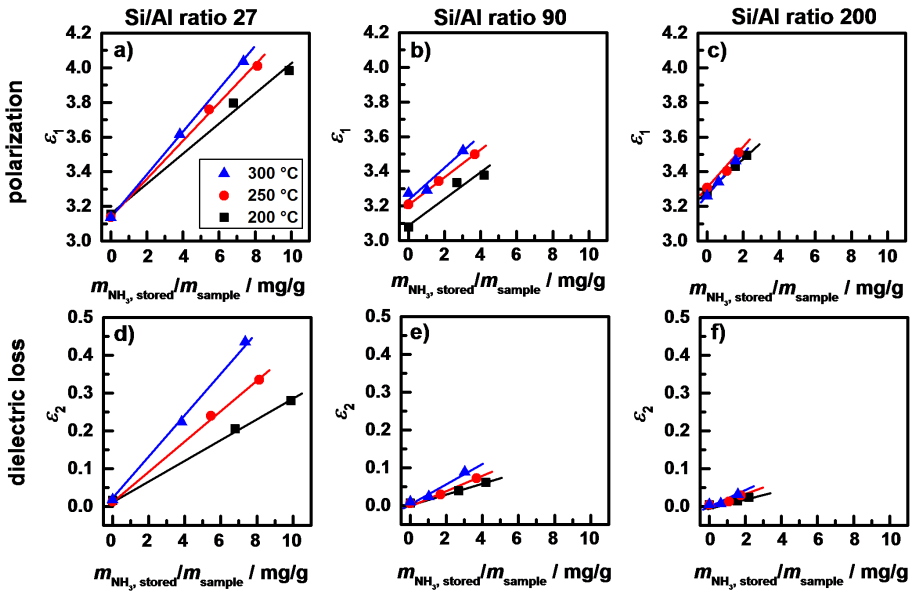

Figure 5. Dielectric permittivity of H-ZSM-5 zeolites as a function of the stored amount of ammonia normalized to the sample mass for different temperatures and Si / Al ratios (27, 90 and 200): **(a)** to **(c)** ε_1, and **(d)** to **(f)** ε_2.

ratios of 27, 90 and 200 are displayed in Fig. 5. The ratio of 800 is excluded since no NH_3 storage could be measured (Fig. 3a), so that the resulting measurement signal is poor. Figure 5a–c show ε_1 and (d) to (f) ε_2 as a function of the normalized stored NH_3 mass at 200, 250 and 300 °C.

The response of ε_1 to NH_3 appears similar for all samples. Completely free of NH_3, ε_1 takes values between 3.1 and 3.3. The variation in these values can be explained by the uncertainties in volume and mass determination in the samples' preparation. For all experiments, ε_1 increases linearly with the stored mass of NH_3 and the rate of increase is similar for all samples. The maximum permittivity value of 4.0 is obtained for the sample with the lowest Si / Al ratio of 27 at the highest temperature of 300 °C. The influence of temperature is visible in increasing sensitivity, especially for the Si / Al ratio of 27. The reason for this is the thermal activation of the NH_4^+ ions, as they become more mobile at higher temperatures. This sensitivity change becomes smaller with increasing Si / Al ratio.

ε_2 increases linearly with the NH_3 content as well, but shows a different dependence on the Si / Al ratio. Without NH_3, ε_2 is almost zero for all samples at all temperatures, as zeolites are low-loss materials. Increasing temperature affects the measured ε_2 significantly, with a higher increase in sensitivity. With an increasing Si / Al ratio, the sensitivity of ε_2 to NH_3 decreases. However, the sensitivity is strongly related to the Si / Al ratio. The highest value for ε_2 of 0.45 was determined for the lowest Si / Al ratio of 27 at 300 °C.

For a closer look at the sensitivity of ε_1 and ε_2 to NH_3, Fig. 6 shows the sensitivities calculated by Eq. (4) as a function of the Al content (corresponding to the given Si / Al ratio) as calculated from the rates shown in Fig. 5. The sensitivity S_1 of ε_1 to NH_3 in Fig. 6a appears to be independent of the Si / Al ratio. The small deviations, especially for the measurements of the Si / Al ratio of 90, result from generally less NH_3 storage with increasing Si / Al ratio and from the consequently higher impact of temperature inconstancies to the small changes of the resonance frequency. The sensitivity S_2 of ε_2 to NH_3 in Fig. 6b increases linearly with the Al content for each temperature and increases with increasing temperature.

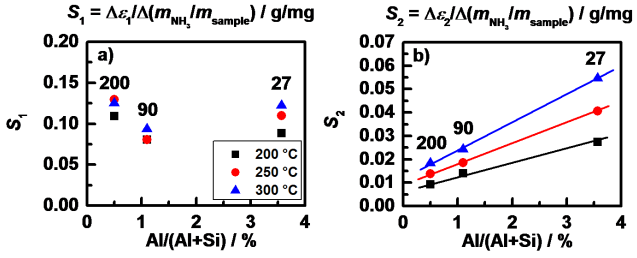

Figure 6. Sensitivities of the dielectric permittivity of H-ZSM-5 zeolites to ammonia: **(a)** S_1 for ε_1, and **(b)** S_2 for ε_2, for Si / Al ratios of 27, 90 and 200 at temperatures of 200, 250 and 300 °C.

$$S_i = \frac{\Delta\varepsilon_i}{\Delta(m_{NH_3} / m_{sample})} i = 1, 2 \quad (4)$$

A possible explanation for these observed dependencies of the sensitivity is that the change in ε_1, as a measure for polarization, is mostly dependent on the stored amount of NH_3, as the NH_3 molecules are highly polar. With higher temperature, the polarity of the NH_3 molecule increases, which is

most visible for the Si / Al ratio of 27 in Fig. 6a. The change in ε_2, which represents the dielectric loss, is strongly dependent on the observed material. It can include conductivity mechanisms (ionic and/or electronic) for conducting samples. With decreasing Al content of the zeolite, the number of the Brønsted acid sites decreases and the distance between them increases. Consequently, the proton mobility due to proton hopping between neighboring Brønsted sites (Rodriguez-Gonzalez et al., 2008) decreases with increasing storage site distance. The part of the dielectric loss related to the proton mobility of the adsorbed NH_3 molecules increases with temperature, resulting in lower activation energies (thermal activation) for proton hopping, corresponding to the observed measurement results.

5 Conclusions and outlook

In this study, initial measurements with a recently introduced measurement setup using microwave cavity perturbation for catalyst powder samples are performed on H-ZSM-5 zeolites with different Si / Al ratios under reaction conditions. The observed temperature range is 200 to 300 °C and all measurements are performed without the influence of humidity. The amount of stored NH_3 is mirrored by both the real ε_1 and the imaginary parts ε_2 of the complex dielectric permittivity. From this we conclude that both values are suitable for NH_3 detection. Through comparison of different Si / Al ratios, ε_1 shows a similar sensitivity to NH_3 for all samples with the same temperature dependence. The sensitivity of ε_2 to NH_3 has a strong dependence on the Si / Al ratio and on temperature. A possible explanation is that the change of ε_1 represents only the polarity of the present NH_3 molecules, and the change of ε_2 is additionally related to the conductivity mechanisms of the zeolite material, for example, by proton hopping.

In future work, the influence of humidity will be observed and ion-exchanged samples will be investigated. Another focus is to further enhance the setup to access a higher temperature range, to incorporate the ability to perform simultaneous temperature-programmed desorption experiments and to increase measurement accuracy. Additionally, frequency-dependent measurements of the complex permittivity by analyzing several cavity modes (from 1.1 to 4.2 GHz) are planned.

Author contributions. M. Dietrich, D. Rauch, A. Porch, and R. Moos conceived and designed the test setup. M. Dietrich performed the experiments and analyzed the data. All authors evaluated the results and wrote the paper.

Acknowledgements. R. Moos is indebted to the German Research Foundation (DFG) for supporting this work under grant MO 1060/19-1.

U. Simon acknowledges financial supported by the German Research Foundation (DFG), contract No: Si609/14-1, and by the Exploratory Research Space of RWTH Aachen University within the Center for Automotive Catalytic Systems Aachen (ACA).

A. Porch acknowledges the support of Merck GKaA.

Edited by: N. Imanaka
Reviewed by: two anonymous referees

References

Beulertz, G., Herbst, F., Hagen, G., Fritsch, M., Gieshoff, J., and Moos, R.: Microwave Cavity Perturbation as a Tool for Laboratory In Situ Measurements of the Oxidation State of Three Way Catalysts, Top. Catal., 56, 405–409, doi:10.1007/s11244-013-9987-3, 2013.

Di Iorio, J. R., Ribeiro, F. H., Bates, S. A., Verma, A. A., Miller, J. T., and Gounder, R.: The Dynamic Nature of Brønsted Acid Sites in Cu–Zeolites During NOx Selective Catalytic Reduction: Quantification by Gas-Phase Ammonia Titration, Top. Catal., 58, 424–434, doi:10.1007/s11244-015-0387-8, 2015.

Dietrich, M., Rauch, D., Porch, A., and Moos, R.: A laboratory test setup for in situ measurements of the dielectric properties of catalyst powder samples under reaction conditions by microwave cavity perturbation: set up and initial tests, Sensors, 14, 16856–16868, doi:10.3390/s140916856, 2014.

Feulner, M., Hagen, G., Moos, R., Piontkowski, A., Müller, A., Fischerauer, G., and Brüggemann, D.: In-Operation Monitoring of the Soot Load of Diesel Particulate Filters: Initial Tests, Top. Catal., 56, 483–488, doi:10.1007/s11244-013-0002-9, 2013.

Franke, M. and Simon, U.: Proton mobility in H-ZSM5 studied by impedance spectroscopy, Solid State Ionics, 118, 311–316, doi:10.1016/S0167-2738(98)00436-6, 1999.

Franke, M. and Simon, U.: Solvate-Supported Proton Transport in Zeolites, Chem. Phys. Chem., 5, 465–472, doi:10.1002/cphc.200301011, 2004.

Fremerey, P., Reiß, S., Geupel, A., Fischerauer, G., and Moos, R.: Determination of the NO_x Loading of an Automotive Lean NO_x Trap by Directly Monitoring the Electrical Properties of the Catalyst Material Itself, Sensors, 11, 8261–8280, doi:10.3390/s110908261, 2011.

Giodanino, F., Borfecchia, E., Lomachenko, K., Lazzarini, A., Agostini, G., Gallo, E., Soldatov, A. V., Beato, P., Bordiga, S., and Lamberti, C.: Interaction of NH_3 with Cu-SSZ-13 Catalyst: A Complementary FTIR, XANES, and XES Study, Journal of Physical Chemistry Letters, 5, 1552–1559, 2014, doi:10.1021/jz500241m, 2014.

Johnson, T. V.: Review of diesel emission and control, Int. J. Engine Res., 10, 275–285, doi:10.1243/14680874jer04009, 2009.

Koebel, M., Elsener, M., and Kleemann, M.: Urea-SCR: a promising technique to reduce NO_x emissions from automotive diesel engines, Catal. Today, 59, 335–345, doi:10.1016/s0920-5861(00)00299-6, 2000.

Kulkarni, V. P., Leustek, M. E., Michels, S. K, Nair, R. N., Snopko, M. A., and Knitt, A. A.: Ash Detection in Diesel Particulate Filter, U.S. Patent 8, 470, 070 B2, 25 June 2013.

Moos, R., Spörl, M., Hagen, G., Gollwitzer, A., Wedemann, M., and Fischerauer, G.: TWC: lambda control and OBD without

lambda probe – an initial approach, SAE paper 2008-01-0916, 2008, doi:10.4271/2008-01-0916, 2008.

Moos, R., Wedemann, M., Spörl, M., Reiß, S., and Fischerauer, G.: Direct Catalyst Monitoring by Electrical Means: An Overview on Promising Novel Principles, Top. Catal., 52, 2035–2040, doi:10.1007/s11244-009-9399-6, 2009.

Moos, R., Beulertz, G., Reiß, S., Hagen, G., Votsmeier, M., Fischerauer, G., and Gieshoff, J.: Overview of the Microwave-Based Automotive Catalyst State Diagnosis, Top. Catal., 56, 358–364, doi:10.1007/s11244-013-9980-x, 2013.

Niwa, M. and Katada, N.: New Method for the Temperature-Programmed Desorption (TPD) of Ammonia Experiment for Characterization of Zeolite Acidity: A Review, Chemical Record, 5, 432–455, doi:10.1002/tcr.201300009, 2013.

Porch, A., Slocombe, D., Beutler, J., Edwards, P., Aldawsari, A., Xiao, T., Kuznetsov, V., Almegren, H., Aldrees, S., and Almaqati, N.: Microwave treatment in oil refining, Applied Petrochemical Research, 2, 37 44, doi:10.1007/s13203-012-0016-4, 2012.

Rahkamma-Tolonen, K., Maunula, T., Lomma, M., Huuhtanen, M., and Keiski, R. L.: The effect of NO_2 on the activity of fresh and aged zeolite catalysts in the NH3-SCR reaction, Catal. Today, 100, 217-222, doi:10.1016/j.cattod.2004.09.056, 2005.

Rauch, D., Kubinski, D., Simon, U., and Moos, R.: Detection of the ammonia loading of a Cu Chabazite SCR catalyst by a radio frequency-based method, Sensor Actuat. B-Chem., 205, 88–93, doi:10.1016/j.snb.2014.08.019, 2014.

Rauch, D., Kubinski, D., Cavataio, G., Upadhyay, D., and Moos, R.: Ammonia Loading Detection of Zeolite SCR Catalysts using a Radio Frequency based Method, SAE Technical Paper 2015-01-0986, doi:10.4271/2015-01-0986, 2015.

Reiß, S., Wedemann, M., Spörl, M., Fischerauer, G., and Moos, R.: Effects of H_2O, CO_2, CO, and flow rates on the RF-based monitoring of three-way catalysts, Sensor Letters 2011, 9, 316–320, doi:10.1166/sl.2011.1472, 2011a.

Reiß, S., Schönauer, D., Hagen, G., Fischerauer, G., and Moos, R.: Monitoring the Ammonia Loading of Zeolite-Based Ammonia SCR Catalysts by a Microwave Method, Chemical Engineering Technology, 34, 791–796, doi:10.1002/ceat.201000546, 2011b.

Rodriguez-Gonzalez, L., Rodriguez-Castellon, E., Jimenez-Lopez, A., and Simon, U.: Correlation of TPD and impedance measurements on the desorption of NH3 from zeolite H-ZSM-5, Solid State Ionics 179, 1968–1973, doi:10.1016/j.ssi.2008.06.007, 2008.

Sappok, A., Parks, J., and Prikhodko, V.: Loading and Regeneration Analysis of a Diesel Particulate Filter with a Radio Frequency-Based Sensor, SAE Technical Paper 2010-01-2126, doi:10.4271/2010-01-2126, 2010.